JOURNAL OF APPLIED ELECTROCHEMISTRY 19 (1989) 51–60

Flow-through and flow-by porous electrodes of nickel foam. II. Diffusion–convective mass transfer between the electrolyte and the foam

S. LANGLOIS, F. COEURET

Laboratoire de Génie des Procédés, CNRS, Ecole Nationale Supérieure de Chimie de Rennes, Avenue du Géneral Leclerc, 35700 Rennes-Beaulieu, France

Received 21 October 1987; revised 15 July 1988

The work described here concerns the diffusion–convective mass transfer to flow-through and flow-by porous electrodes of nickel foam. Empirical correlations giving the product $\bar{k}_d a_e$ of the mass transfer coefficient $\bar{k}_d$ and the specific surface area a_e of the material as a function of the pressure drop per unit electrode height and as a function of the grade characterizing the foam are proposed. The performance of various materials are compared in terms of $\bar{k}_d a_e$ vs the mean linear electrolyte flow velocity.

Nomenclature

a_e	specific surface area (per unit of total volume of electrode) (m^{-1})
A, B	Ergun law coefficients determined in flow-by configuration
A', B'	Ergun law coefficients determined in flow-through configuration A, A' ($Pa\,m^{-3}\,s^2$); B, B' ($Pa\,m^2\,s^{-1}$)
C_E	entering concentration of ferricyanide ions ($mole\,m^{-3}$)
D	molecular diffusion coefficient ($m^2\,s^{-1}$)
F	Faraday number ($C\,mol^{-1}$)
G	grade of the foams
I_L	limiting current (A)
$\bar{k}_d$	mean mass transfer coefficient ($m\,s^{-1}$)
n	number of stacked foam sheets in the electrode
$\Delta P/H$	pressure drop per unit of height ($Pa\,m^{-1}$)
Q_v	volumetric electrolyte flow rate ($m^3\,s^{-1}$)
Re	Reynolds number
Sc	Schmidt number
Sh	Sherwood number
T	mean tortuosity of the foam pores
$\bar{u}$	mean electrolyte velocity ($m\,s^{-1}$)
V_R	electrode volume (m^3)
X	conversion
μ	dynamic viscosity ($kg\,m^{-1}\,s^{-1}$)
v_e	number of electrons in the electrochemical reaction
ν	kinematic viscosity ($m^2\,s^{-1}$)

1. Introduction

In Part I [1] three nickel foams with the grade 100, 60 and 45 (and denoted G100, G60 and G45, respectively), were characterized from the standpoint of application as electrode materials for flow-through or flow-by porous electrodes. Produced in France by SORAPEC [2], such foams have particular properties (high porosity, small apparent electrical resistivity, high specific surface area, quasi-isotropy) which make them potentially interesting as porous electrodes for the electrolytic treatment of dilute solutions. A preliminary experimental mass transfer study was made with flow-through porous electrodes of nickel felt and nickel foam, but these materials were not geometrically and physically characterized [3]. This study highlighted the need for more extensive work on the possibilities of nickel foam electrodes. Let us recall that the foams are commercially designated by the value of the grade which is the number of pores per linear inch (ppi).

It is well known that the value of the mass transfer coefficient in given hydrodynamic conditions is necessary for the determination of the minimum electrode size. Mass transfer between a liquid in forced flow and the three foams characterized in [1] was studied with an experimental procedure analogous to that of [3]. The foams were considered as flow-by porous electrodes (electrical current normal to the electrolyte flow) and as flow-through porous electrodes (electrical current parallel to the electrolyte flow).

The present Part II gives the results of this mass transfer study and compares the performances of the nickel foams to that of other electrode materials. Part III [4] will discuss the electrode potential distributions within both electrode configurations studied here.

2. Mass transfer at flow-by porous electrodes

2.1. *Experimental details*

Diffusional mass transfer was studied at electrodes constructed with only one sheet of nickel foam and with various sheets (stacked electrodes). Let us recall

0021-891X/89 $03.00 + .12

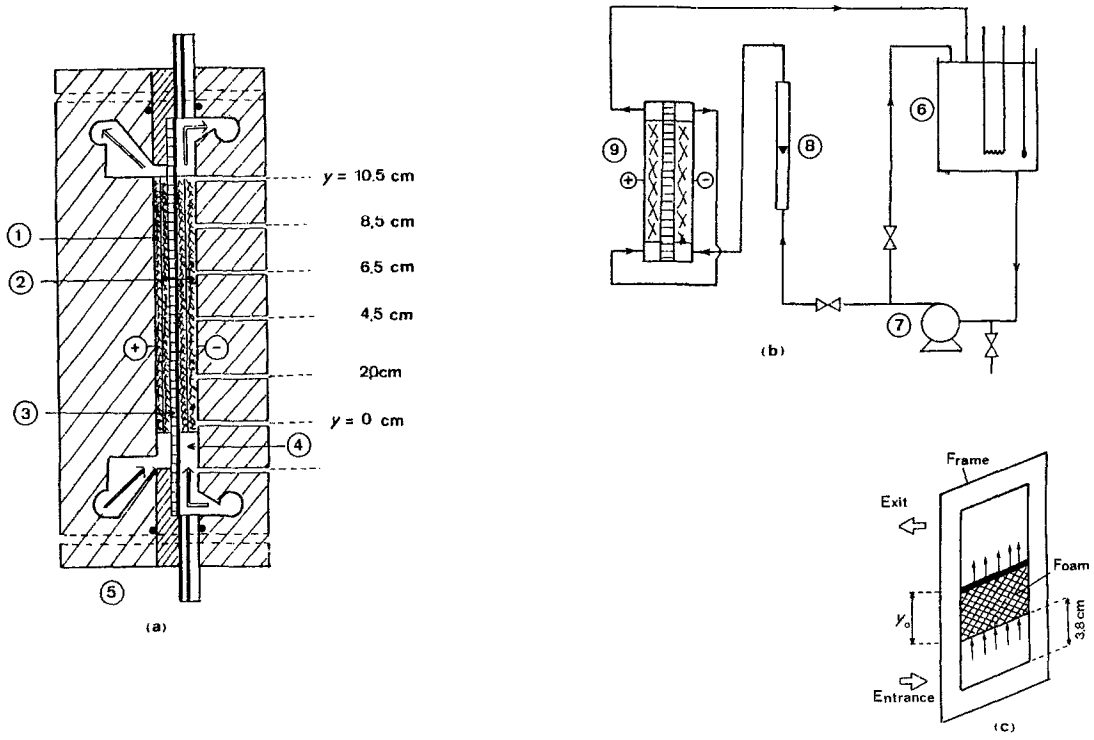

Fig. 1. Views of the cell (a), of the hydraulic circuit (b), and of a frame supporting a foam. 1, Anode (stack of nickel foam); 2, cathode (stack of elements as in scheme (c)); 3, porous separator and membrane; 4, calming section; 5, frames supporting the foams; 6, reservoir; 7, centrifugal pump; 8, rotameter; 9, cell.

that sheet (approximately 0.0025 m thick) is the commercially available form of the nickel foam [1, 2]. Thus, flow-by electrodes of different thickness were studied. The physical and geometrical properties of the three nickel foams G100, G60 and G45 were given in [1].

The electrolytic cell is represented in Fig. 1a while Fig. 1b shows the hydraulic circuit and Fig. 1c gives a schematic view of one sheet of foam on its support and current feeder. The two-compartment cell is parallelepipedic and made of Altuglas; the two compartments are separated by a cation exchange membrane (Selemion CMV 10) which is supported by a porous polyethylene separator (Vyon "F").

The cathodic compartment is defined by the stack of the frames on which the individual foam electrodes are fixed, and by the intermediate rubber joints. Each frame (Fig. 1c) is rectangular; it is made of stainless steel 0.001 m thick and the dimensions of the rectangular hole are 0.07 m × 0.17 m. The foam of height y_0 is electrically soldered onto the frame, which acts as the current feeder to the foam; the lower part of the foam electrode (entrance plane of the liquid in the foam) is always located at the same distance (0.038 m) from the lower smaller side of the frame. The following electrode heights, y_0, were used: 0.025, 0.05, 0.07, 0.09 and 0.115 m. The parts of the frame which contact the liquid are coated with a protective laquer (M-coat D from Vishay Micromesures).

The electrolyte enters and leaves the cell through the cover of the cathodic compartment itself, in which rectangular slot distributors are machined (see Fig. 1a). Plastic foam is located within the entrance distributor in order to make the velocity profile uniform. As indicated in Fig. 1a, the cover of the cathodic compartment carries 7 cylindrical holes with tight caps for the introduction of capillary pressure taps; one of these holes is used for the control of the cathodic electrode potential. The anodic compartment is 0.007 m deep; a stack of 3 sheets of nickel foam is located within this compartment and works as the anode.

The electrolyte flows in a closed circuit, through the cathodic and the anodic compartments successively (Fig. 1b). Its temperature is maintained at 30° C in the reservoir in which a continuous bubbling of nitrogen takes place for the elimination of dissolved oxygen.

The composition and the properties of the electrolyte are given in Table 1; this electrolyte allows mass transfer to be studied at the nickel foam by means of the reduction of the ferricyanide ions. The high ratio between the $K_4Fe(CN)_6$ and $K_3Fe(CN)_6$ concentrations allows oxygen evolution at the anode to be avoided and convective-diffusion limitation at the cathode only. The concentration of the ferricyanide ions is

Table 1. Properties of the electrolyte

Composition	NaOH 1 N $K_4Fe(CN)_6$ 0.125 M $K_3Fe(CN)_6$ 0.0025 M
Temperature	30° C
Density	$\varrho = 1.07 \times 10^3$ kg m^{-3}
Kinematic viscosity	$\nu = 1.005 \times 10^{-6}$ m^2 s^{-1}
Dynamic viscosity	$\mu = 1.071 \times 10^{-3}$ kg m^{-1} s^{-1}
Diffusion coefficient of ferricyanide	$D = 6.4 \times 10^{-10}$ m^2 s^{-1}
Schmidt number	$Sc = \nu/D = 1570$

established by amperometric titration with a rotating platinum disk electrode using cobalt sulphate.

The electrical circuit is a classical three-electrode potentiostatic circuit using a Tacussel PRT 20-2 potentiostat. The current–potential curves give a well-defined horizontal plateau over the range of variation of the electrolyte flow velocity $\bar{u}$ which is based on the cross-sectional area of the empty cathodic compartment.

2.2. *Theoretical aspects*

From the limiting diffusion current, I_L, at a given cathode percolated by the flow rate, Q_v, with entering ferricyanide concentration, C_E, the conversion, X, of the ferricyanide ions is calculated from the following expression:

$$X = \frac{I_L}{v_e F Q_v C_E} \tag{1}$$

which supposes a faradic yield of one, and in which $v_e(= 1)$ is the number of electrons in the electrochemical reaction and F the Faraday number.

If the plug-flow model applies to diffusional mass transfer at the porous electrode, the mass transfer coefficient, $\bar{k}_d$, between the flowing electrolyte and the matrix of the electrode depends on X through the following expression:

$$\bar{k}_d a_e = -\frac{Q_v}{V_R} \ln (1 - X) = -\frac{\bar{u}}{y_0} \ln (1 - X) \tag{2}$$

where a_e is the electrode surface area per unit volume of electrode and V_R the electrode volume [5]. Let us recall that a distinction has to be made between the static specific surface area and the dynamic specific surface area [1]. Here a_e is the electrochemically active specific surface area. Its value may be different from both the above-mentioned specific surface areas, but generally it is not possible to know it. This is not a problem for design because, as shown by Equation 2, $\bar{k}_d$ and a_e do not have to be known separately but only as the product $\bar{k}_d a_e$.

In the present paper all the mass transfer results are presented in the form of $\bar{k}_d a_e$.

2.3. *Mass transfer at a sheet of nickel foam*

The electrode thickness is constant for a given foam and approximately equal to 0.0025 m (see Table 2 of [1]).

The values of X calculated through Equation 1 are plotted in Fig. 2 as log $(1 - X)$ vs y_0 for electrolyte velocities $\bar{u}$ varying between 0.015 and 0.13 m s^{-1}. It is seen that the form of expression 2 is verified, which confirms that the electrodes behave approximately as piston-flow reactors. At a given value of $\bar{u}$ the foam G100 leads to a conversion twice as higher as with foam G45 having the same height y_0. A foam G100 0.1 m high gives a conversion X higher than 0.6 for $\bar{u} = 0.02$ m s^{-1}, a result which confirms the favourable behaviour of these materials. Moreover, by extrapolating the lines of Fig. 2 one may see that, also for $\bar{u} = 0.02$ m s^{-1}, a conversion of 90% would be obtained with an electrode of foam G100 0.25 m high. Thus it is clear that cells giving very high space-time yields can be obtained using metallic foams as the electrode material.

The values obtained for $\bar{k}_d a_e$ from Equation 2 are plotted vs $\bar{u}$ in Fig. 3. Except for the case of foam G100 for which the shorter electrode ($y_0 = 0.025$ m) leads to results very different from those for the other electrode heights, it is not possible to differentiate between

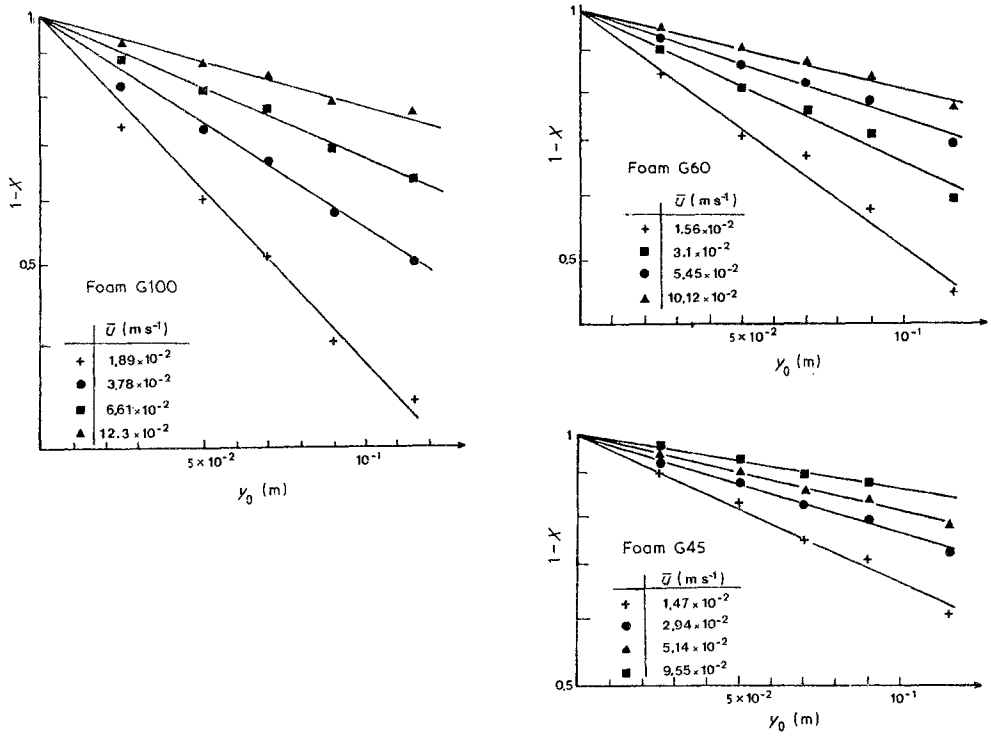

Fig. 2. Variation of $1 - X$ with $\bar{u}$ and y_0.

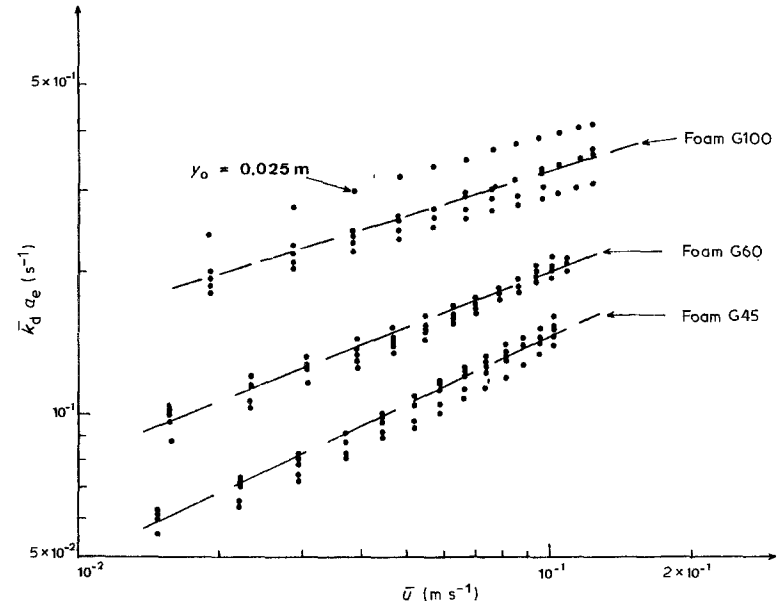

Fig. 3. Variation of $\bar{k}_d a_e$ with $\bar{u}$ for various electrode thickness (flow-by configuration).

the values of y_0. This is the reason why a unique empirical correlation is proposed between $\bar{u}$ and the corresponding mean arithmetic values of $\bar{k}_d a_e$ for all the electrode heights of one category of foam. The lines of Fig. 3 obey the following expressions:

$$\text{foam G100: } \bar{k}_d a_e = (0.69 \pm 0.17) \times (\bar{u})^{0.32} \quad (3a)$$

$$\text{foam G60: } \bar{k}_d a_e = (0.51 \pm 0.05) \times (\bar{u})^{0.39} \quad (3b)$$

$$\text{foam G45: } \bar{k}_d a_e = (0.42 \pm 0.04) \times (\bar{u})^{0.46} \quad (3c)$$

where the units of $\bar{k}_d a_e$ are s^{-1} and those of $\bar{u}$ are m s^{-1}. For the same range of variation of $\bar{u}$ as in the present experiment, the pressure drop measurements showed that the hydrodynamic behaviour of the three foams was different [1]; such a difference is again found here through the exponents of G100 (exponents 1/3) while the transition flow regime prevails for foam G45 (exponent approximatively equal to 0.5).

It was established [6, 7] that the mass transfer coefficient $\bar{k}_d$ is related to the pressure drop per unit of height of the porous medium, $\Delta P/H$, according to the following expression:

$$\bar{k}_d = \text{constant} \times \frac{D^{2/3}}{\mu^{1/3}} \left(\frac{\Delta P}{H}\right)^{1/3} \quad (4)$$

where D is the molecular diffusion coefficient of the

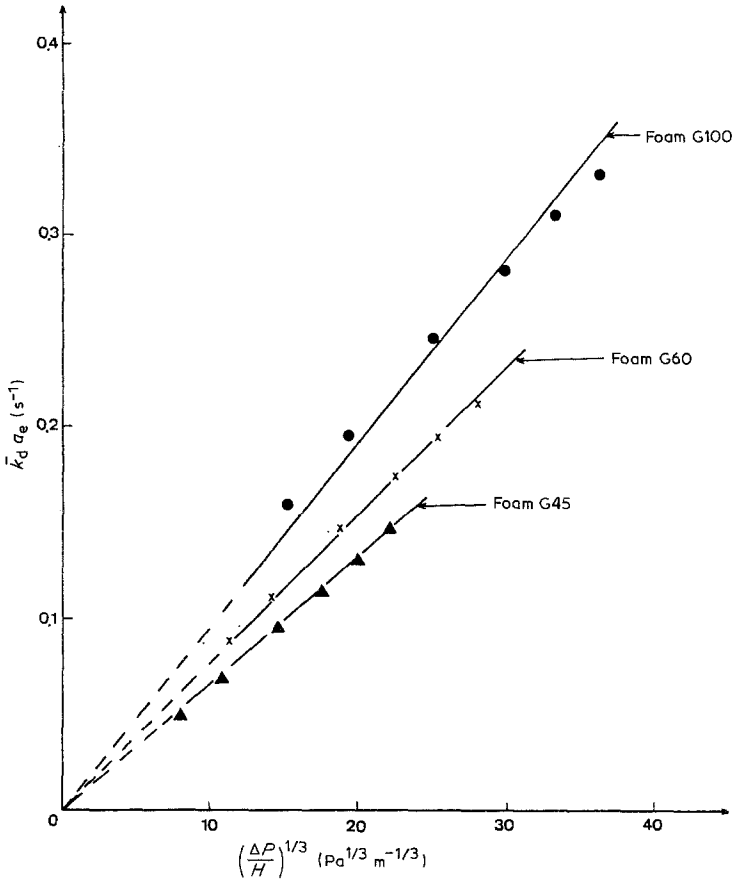

Fig. 4. Variation of $\bar{k}_d a_e$ with $(\Delta P/H)^{1/3}$ (flow-by configuration).

Table 2. Values of the constants $\bar{A}$ and $\bar{B}$ of expression 5

	$\bar{A}$ ($Pa\ m^{-3}\ s^{-2}$)	$\bar{B}$ ($Pa\ m^{-2}\ s^{-1}$)
Foam G100	16.2×10^5	3.4×10^5
Foam G60	9.8×10^5	1.3×10^5
Foam G45	6.2×10^5	5×10^4

transported ions and μ the dynamic viscosity of the liquid.

Expression 4 follows from dimensional analysis and applies independently of the nature of the flow regime; it expresses the relation between wall to liquid mass transfer and mechanical energy losses. Values of $\bar{k}_d a_e$ from correlations of Fig. 4 as a function of the values of $(\Delta P/H)^{1/3}$ calculated for the corresponding values of $\bar{u}$, from the following expression:

$$\frac{\Delta P}{H} = \bar{A}(\bar{u})^2 + B\bar{u} \qquad (5)$$

which obeys the Ergun law and which was previously tested in [1]; the coefficients $\bar{A}$ and $\bar{B}$ for the three foams are recalled in Table 2. Figure 4 shows that the form of Equation 4 applies for the nickel foams (as it probably does for any reticulated structure), and that the slope of the lines increases with the grade [1]. From the slopes of the lines of Fig. 4, the following empirical expression may be obtained:

$$\bar{k}_d a_e = 155(\text{grade})^{0.45} \frac{D^{2/3}}{\mu^{1/3}} \left(\frac{\Delta P}{H}\right)^{1/3} \qquad (6)$$

for the velocity range $0.015\,m\,s^{-1} \leqslant \bar{u} \leqslant 0.13\,m\,s^{-1}$. Thus for this velocity range and foams whose grade value is between 45 and 100, expression 6 permits the calculation of $\bar{k}_d a_e$ from the measurement of the pressure drop per unit height of electrode.

2.4. *Mass transfer at stacks of various sheets of nickel foam*

As only a few pores exist through the thickness of one sheet of foam, it is possible that a wall effect could have affected the mass transfer results obtained at one ($n = 1$) sheet electrode. Thus, mass transfer experiments with stacks of sheets were necessary. Electrodes having the same height ($y_0 = 0.11$ m) and constructed by superposing $n = 2$ or 3 sheets of nickel foam were used; the values of $\bar{k}_d a_e$ are plotted as a function of $\bar{u}$ in Fig. 5.

It is observed in Fig. 5 that the results do not depend on n, in spite of the extension of the velocity range towards small values of $\bar{u}$. The lines drawn in Fig. 5 correspond to the following empirical correlations:

$$\text{foam G100: } \bar{k}_d a_e = 1.26(\bar{u})^{0.48} \qquad (7a)$$

$$\text{foam G60: } \bar{k}_d a_e = 0.61(\bar{u})^{0.45} \qquad (7b)$$

$$\text{foam G45: } \bar{k}_d a_e = 0.43(\bar{u})^{0.47} \qquad (7c)$$

established with a correlation coefficient of 0.98 for $\bar{u}$ varying from $0.005\,m\,s^{-1}$ to $0.1\,m\,s^{-1}$.

The exponent of $\bar{u}$ is nearly 0.5 for the three foams and the overall behaviour of the foams is the same, a conclusion which disagrees with the observation made in [1] concerning pressure drop measurements through only one sheet of foam. The result of Fig. 5 lead to the following empirical correlation:

$$\bar{k}_d a_e = (2.5 \pm 0.3) \times 10^{-3}\,(\text{grade})^{1.35}\,(\bar{u})^{0.47} \qquad (8)$$

for $n = 1$, 2 or 3, $0.005\,m\,s^{-1} \leqslant \bar{u} \leqslant 0.1\,m\,s^{-1}$, and for foams such that $45 \leqslant$ grade $\leqslant 100$. The dimensions of $\bar{k}_d a_e$ and $\bar{u}$ in Equation 8 are s^{-1} and $m\,s^{-1}$, respectively.

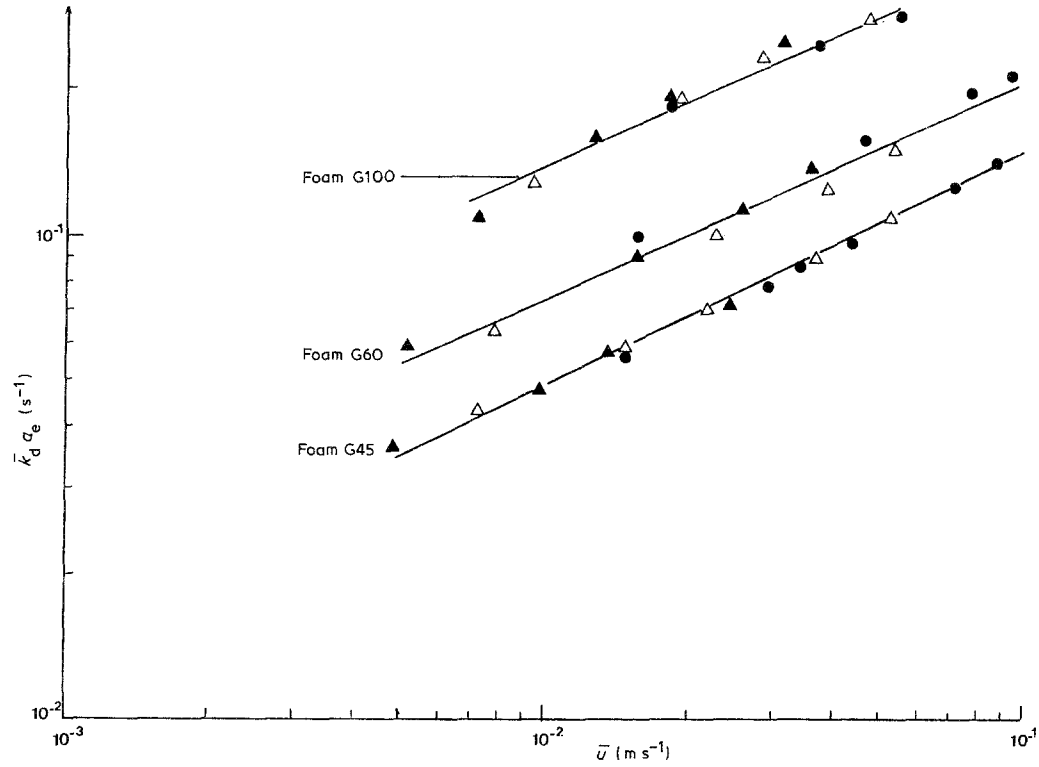

Fig. 5. Variation of $\bar{k}_d a_e$ with $\bar{u}$ for the three foams (flow-by configuration). ● $n = 1$, △ $n = 2$, ▲ $n = 3$.

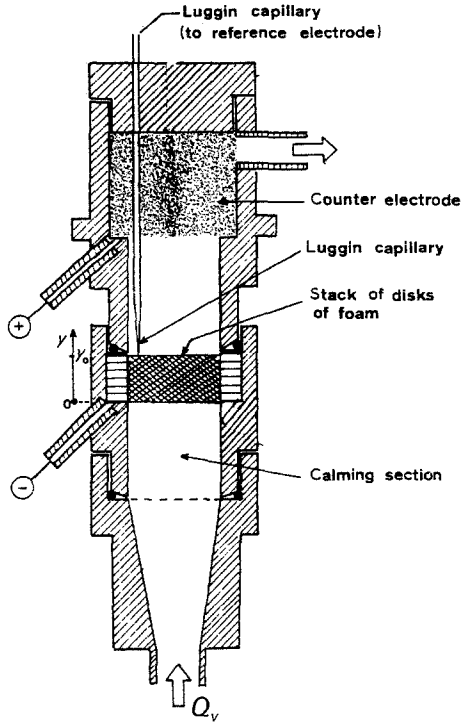

Fig. 6. View of the cell used for the study of flow-through porous electrodes.

Dimensional analysis shows that expression 8 agrees with the usual form of mass transfer correlations between dimensionless numbers, for example Sh = constant × $Re^m Sc^{1/3}$. Indeed, as the grade has the dimension of a specific surface area, i.e. that of the inverse of a pore diameter [1], expressions giving the Sherwood number can lead to:

$$\bar{k}_d a_e = \text{constant (grade)}^{2-m} (\bar{u})^m$$

which agrees with the form of Equation 8, the constant being a function of the viscosity and the diffusivity.

3. Mass transfer at flow-through porous electrodes

3.1. *Experimental details*

Mass transfer experiments were undertaken with flow-through porous electrodes in order to extend the explored variation range of $\bar{u}$ to smaller values and also to obtain the mass transfer performance of nickel foam electrodes for small heights in the electrolyte flow direction. The experimental method used is the same as that described previously in [3] where details on the electrode construction may also be found.

The column used is shown in Fig. 6. It is cylindrical (internal diameter 0.04 m), made of Altuglas and consists of three parts: a calming section of glass spheres, a central part containing the stack of n ($1 \leqslant n \leqslant 6$) circular disks of nickel foam, and an upper part containing the counter electrode (stack of disks of foam G100). The electrode potential at the top of the stack, i.e. at $y = y_0$, is imposed by means of a Luggin capillary connected to a saturated calomel reference electrode. The stack contained in the central part of the column acts cathodically and the limiting diffusion current at this stack is obtained using the cathodic reduction of potassium ferricyanide. The properties of the electrolyte used are those given in Table 1. As in [3], the electrolyte flows in a closed circuit and the procedure uses a three-electrode potentiostatic electrical circuit.

3.2. *Results and empirical correlation*

As for the flow-by porous electrodes (Fig. 2), it was demonstrated here from the mass transfer results that the stack of disks of nickel foam behaves as an electrochemical plug flow reactor [8]. The difficulties generated in [3] by the retention of air bubbles within the porous bed were much smaller in the present work, the reason being that the foam texture was less dense than in [3]. However it was necessary to take precautions against accumulation of air bubbles during the filling of the hydraulic circuit.

Figure 7 presents the variations of $\bar{k}_d a_e$, also deduced from Equation 2 as previously, as function of the mean electrolyte flow velocity in the empty column, $\bar{u}$. The results are given for different stacks of the three foams. For $n = 1$, the values of $\bar{k}_d a_e$ are always higher than those corresponding to other values of n. At a given velocity $\bar{u}$, and for a particular foam, the maximum deviation between the extreme values of $\bar{k}_d a_e$ is about $\pm 25\%$.

By considering the arithmetic mean value of $\bar{k}_d a_e$ for the 6 stacks at each $\bar{u}$ value, the following empirical expressions are obtained in the velocity range $0.002\,\text{m s}^{-1} \leqslant \bar{u} \leqslant 0.02\,\text{m s}^{-1}$:

$$\text{foam G100: } \bar{k}_d a_e = (0.80 \pm 0.08)(\bar{u})^{0.30} \quad (9a)$$

$$\text{foam G60: } \bar{k}_d a_e = (0.28 \pm 0.03)(\bar{u})^{0.30} \quad (9b)$$

$$\text{foam G45: } \bar{k}_d a_e = (0.075 \pm 0.01)(\bar{u})^{0.22} \quad (9c)$$

with $\bar{k}_d a_e$ expressed in s^{-1} and $\bar{u}$ in m s^{-1}.

Figure 8 compares correlations 7 and 9 which are established for two electrode configurations and for partially identical ranges of $\bar{u}$.

It is seen that: (a) the exponents of $\bar{u}$ are smaller for the flow-through configuration than for the flow-by configuration, and the exponent of 0.30 in Equation 9 agrees with the existence of a viscous flow regime within the porous structure; (b) the deviations between correlations 9 are higher than between correlations 7; (c) for a given foam (as for example for foams G100 and G45) there are sometimes large deviations between the correlations corresponding to the two configurations; (d) from the results of Fig. 7 it is not possible to propose a unique empirical correlation analogous to Equation 8 because there is no common value of the slopes.

3.3. *Analysis from pressure drop measurements*

Experimental measurements of the static pressure drop of the liquid flowing in forced flow through a stack of about 50 circular disks of nickel foam were made in a separated cylindrical column (internal

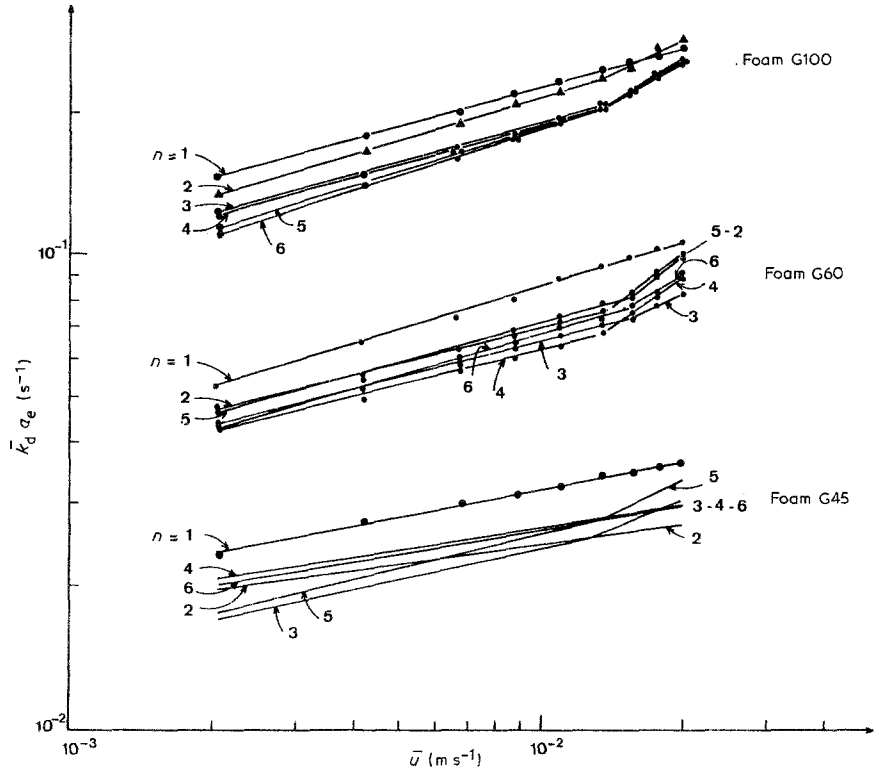

Fig. 7. Variation of $\bar{k}_d a_e$ with $\bar{u}$ for various electrode thickness (flow-through configuration).

diameter 0.024 m). The height of each stack was about 0.1 m and the mean liquid velocity $\bar{u}$ in the empty column was varied between 0.005 m s^{-1} and 0.05 m s^{-1}. As schematically shown in Fig. 9, 6 pressure taps were regularly located all along the column, thus making possible pressure drop measurements through various vertical distances, H, to the lower pressure tap.

As presented in Fig. 9 for foam G100, the pressure drop ΔP can be expressed as:

$$\frac{\Delta P}{H\bar{u}} = A'(\bar{u} - \bar{u}_0) + B' \qquad \text{when } \bar{u} \geqslant \bar{u}_0 \qquad (10a)$$

$$\frac{\Delta P}{H\bar{u}} = B' \qquad \text{when } \bar{u} \leqslant \bar{u}_0 \qquad (10b)$$

The values of $\bar{A}'$ and $\bar{B}'$ are given in Table 3 for the three foams. The velocity $\bar{u}_0$, the value of which is about 0.02 m s^{-1} whatever the foam, is the liquid velocity at which the inertial flow regime is established. This supports the idea that for the flow-through configuration (Fig. 8), the flow regime corresponding to $\bar{u}$ values smaller than $\bar{u}_0$ would be laminar viscous. This is also supported by the exponent of $\bar{u}$ in Equation 9.

For the flow-through configuration, Fig. 10 gives the variations of $\bar{k}_d a_e$ as function of $(\Delta P/H)^{1/3}$; as the

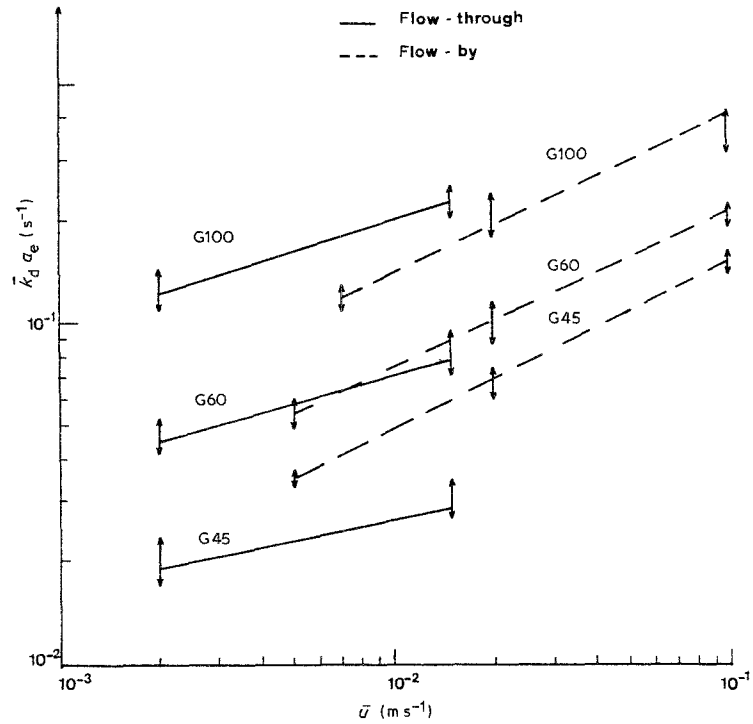

Fig. 8. Comparison of the mass transfer correlations obtained with the two electrode configurations.

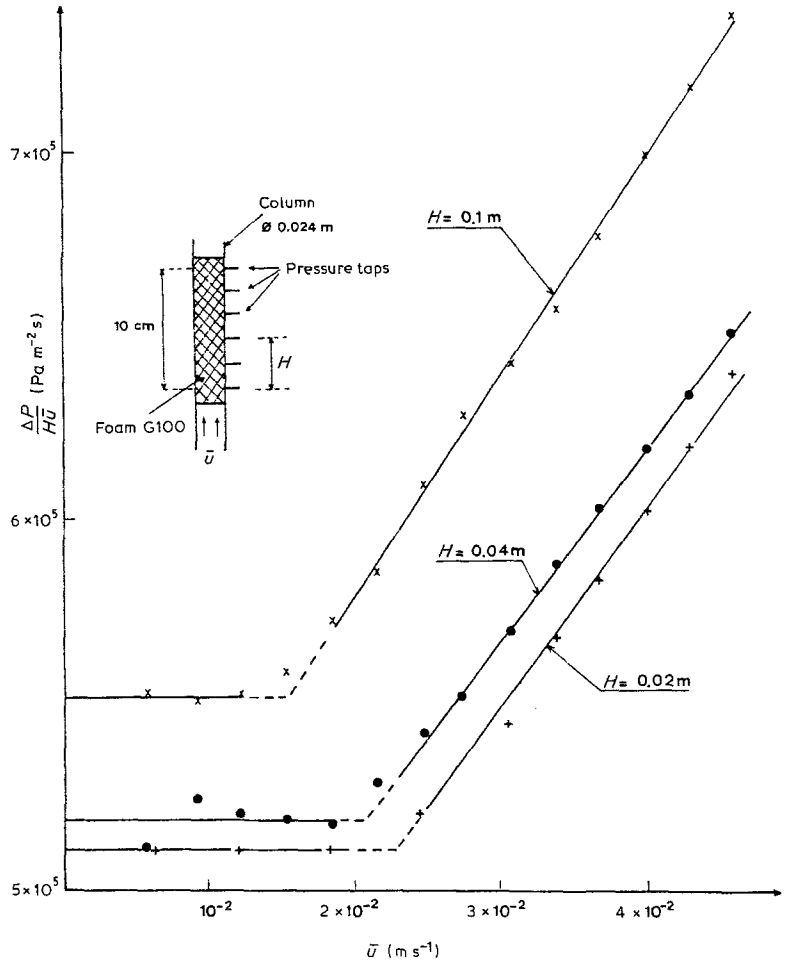

Fig. 9. Variations of $\Delta P/(H\bar{u})$ with $\bar{u}$ for the flow through a cylindrical stack of disks of foam G100.

mass transfer measurements are made for the viscous flow regime, $\Delta P/H$ is calculated from Equation 10b. A linear dependence is observed in Fig. 10 and from the slopes of the three straight lines, the following relation between mass transfer and mechanical energy loss can be proposed for nickel foams of 45 $\leqslant$ grade $\leqslant$ 100 and for the velocity range $0.002\,\mathrm{m\,s^{-1}} \leqslant \bar{u} \leqslant 0.02\,\mathrm{m\,s^{-1}}$:

$$\bar{k}_d a_e = 0.53(\text{grade})^{1.75} \times \frac{D^{2/3}}{\mu^{1/3}} \left(\frac{\Delta P}{H}\right)^{1/3} \quad (11)$$

The dimensions of the different terms of Equation 11 are those given in the nomenclature.

4. Discussion

The differences between the mass transfer results obtained for the two configurations may be analysed through the comparison of the pressure drops.

One notes that the values of $\bar{A}'$ and $\bar{B}'$ of Equation 10 (see Table 3) are higher than the values of $\bar{A}$ and $\bar{B}$ of Equation 5 (see Table 2). Thus, for a given electrolyte velocity $\bar{u}$ the pressure drop per unit of height, $\Delta P/H$, is higher for the flow-through (Fig. 6) configuration. The ratio $\bar{A}'/\bar{A}$ is about 3 while the ratio $\bar{B}'/\bar{B}$ is about 1.5.

Table 3. Values of the constants $\bar{A}'$ and $\bar{B}'$ of expression 10

	$\bar{A}'$ ($Pa\,m^{-3}\,s^{-2}$)	$\bar{B}'$ ($Pa\,m^{-2}\,s^{-1}$)	$\bar{A}'/\bar{A}$	$\bar{B}'/\bar{B}$
Foam G100	5.5×10^6	5.3×10^5	3.4	1.6
Foam G60	3.4×10^6	2.4×10^5	3.5	1.8
Foam G45	1.85×10^6	7.5×10^4	3.0	1.5

In [1], the constants $\bar{A}$ and $\bar{B}$ were established; if T is the overall mean tortuosity of the pores, $\bar{A}$ and $\bar{B}$ are proportional to $T^4 a_e$ and $T^2 a_e^2$, respectively. Thus the values of $\bar{A}'$ and $\bar{B}'$ correspond to a situation for which the tortuosity and the dynamic specific surface area would be respectively increased to $1.6\,T$ and lowered to $0.8 a_e$. An explanation can be found in the following manner.

(i) There is a slight anisotropy of the texture of the foams studied [1].

(ii) There is logically a difference between the apparent overall tortuosity of the foam located as a sheet in a rectangular thin channel (0.002 m thick) and as a long cylinder in a column of internal diameter 0.024 m. In the thin rectangular channel, wall effects may induce preferential pathways for the liquid flow.

(iii) Principally for the case of foam G45, there is a slight progressive retention of air within the flow-through porous electrode, particularly at the boundaries between adjacent disks of foam. The presence of gas bubbles at these boundaries probably changes the electrochemically active area at these places and could be responsible for local micromixing.

However, the differences between the behaviour of the two porous electrode configurations have to be considered keeping in mind the fact that the velocity

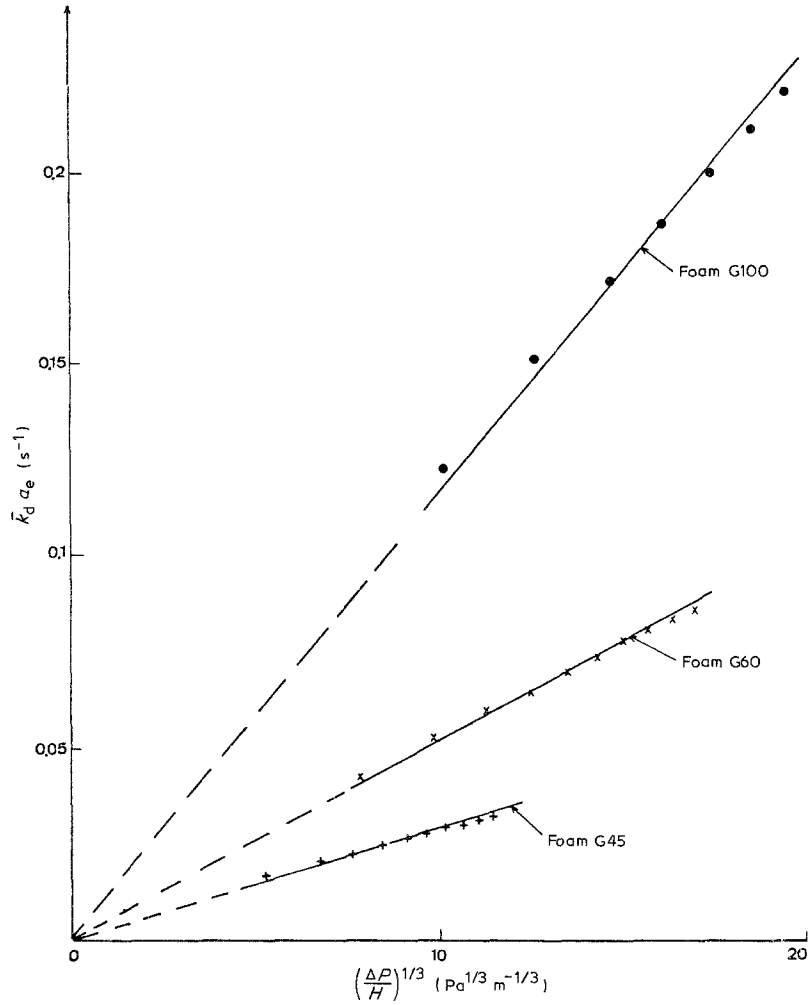

Fig. 10. Variations of $\bar{k}_d a_e$ with $(\Delta P/H)^{1/3}$ (flow-through configuration).

range around 0.01 m s^{-1}, where the deviations are observed between the corresponding correlations (Fig. 8), corresponds to a transition flow regime.

5. Comparison between mass transfer results at the foams and published mass transfer data for other materials

Generally, a comparison of the mass transfer performance of flow-through or flow-by porous electrodes consists of the comparison of empirical correlations involving dimensionless numbers such as the Sherwood number, *Sh*, the Chilton–Colburn j_D factor, the Reynolds number, *Re*, etc. However, in many cases the true electrochemically active surface areas are not known, thus making it difficult or even impossible to define a characteristic dimension needed for the calculation of these dimensionless numbers. Beyond the present case of nickel foams, expanded metals, metallic nets and felts, etc. pose similar problems. This is the reason why it is convenient to compare mass transfer performances in terms of the variation of the product $\bar{k}_d a_e$ as a function of the mean electrolyte velocity $\bar{u}$; indeed, as seen before, this product is directly experimentally accessible. Such a comparison applied to graphite felt and cloth was made by Oren and Soffer [9]. Such an approach is similar to that used in chemical engineering for the comparison of the performances of liquid–liquid or gas–liquid exchangers in which the true interfacial area is generally unknown.

Different materials were considered in the comparison made in Fig. 11. One may see that the values of $\bar{k}_d a_e$ vary over a range of 4 powers of ten while the velocity range is between 0.0001 and 0.1 m s^{-1}. Several points follow from Fig. 11.

(i) The data obtained with nickel foams [3, 8, present work] agree with those published on copper foams [10] and on RVC [11, 17].

(ii) The performance of the foams appears intermediate between those of metallic nets [12] and those of grids of expanded metals having a common lozenge mesh [4, 13].

(iii) The foams are comparable to fixed beds of spherical particles of 1 mm diameter [14], to micromesh-type expanded metal electrodes [4, 13], to electrodes chemically modified from RVC [15] and to fixed beds of small square nickel plates [18].

(iv) The microporous membranes [16] and the graphite [9] or nickel felts [3] perform best but their use probably remains limited to flow-through porous electrodes of small thickness. Also, the compressibility of the felts and the capillary fibre texture of the nickel felts are disadvantages.

Various materials are now available for the construction of flow-through and flow-by porous electrodes. However the technical adaptation, and particularly the need to feed in the current and to stack materials,

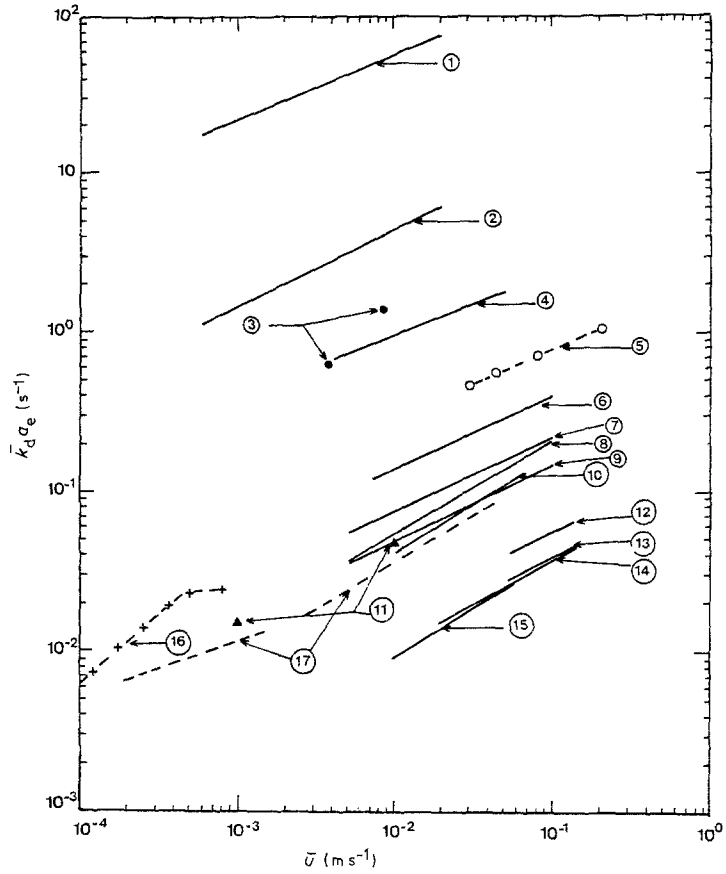

Fig. 11. Comparison of the performances of various materials for flow-through or flow-by porous electrodes. 1, Microporous membrane ($a_e = 1.6 \times 10^5\ m^{-1}$) [16]; 2, microporous membrane ($a_e = 3 \times 10^4\ m^{-1}$) [16]; 3, graphite felt [9]; 4, nickel felt [3]; 5, nickel net ($a_s = 157\ m^{-1}$) [12]; 6, nickel foam G100 [8, present work] (flow-by); 7, nickel foam G60 [8, present work] (flow-by); 8, nickel spheres, $d_p = 0.002$ m [14]; 9, nickel foam G45 [8, present work] (flow-by); 10, expanded metal (micromesh) [5, 13]; 11, chemically modified electrode ($a_e = 8 \times 10^3\ m^{-1}$) [15]; 12, copper foam (20 ppi) [10]; 13, copper foam (10 ppi) [10]; 14, expanded metal (standard mesh) flow-by [5, 13]; 15, expanded metal (standard mesh) flow-through [5, 13]; 16, RVC (100 ppi) [11, 17]; 17, fixed bed of small square (side 5 mm; thickness 1 mm) [18].

may present difficulties with some materials. Among these numerous materials, the metallic foams are undoubtedly very interesting for porous electrode applications.

The following paper will be concerned with the potential distribution within flow-through and flow-by porous electrodes of metallic foam working in limiting diffusion current conditions [4].

Acknowledgements

The authors thank the Direction des Etudes et Recherches d'Electricité de France for its financial support during this work and the Society SORAPEC for the free supply of the materials.

References

[1] S. Langlois and F. Coeuret, *J. Appl. Electrochem.* **19** (1988) 43.
[2] Société SORAPEC, 94129 Fontenay Sous Bois, France.
[3] J. M. Marracino, F. Coeuret and S. Langlois, *Electrochim. Acta* **32** (1987) 1303.
[4] S. Langlois and F. Coeuret, *J. Appl. Electrochem.* (to be submitted).
[5] F. Coeuret and A. Storck, Elements de Génie Electrochimique, Tec-Doc, Lavoisier, Paris (1984).
[6] A. Storck, Thèse de Doctorat d'Etat, INPL, Nancy, France (1976).
[7] A. Storck and F. Coeuret, *Chem. Engng J.* **20** (1980) 149.
[8] S. Langlois, Thèse de Doctorat, Université de Rennes (1988).
[9] Y. Oren and A. Soffer, *Electrochim. Acta* **28** (1983) 1649.
[10] A. Tentorio and U. C. Ginelli, *J. Appl. Electrochem.* **28** (1978) 195.
[11] M. Matlosz and J. Newman, *J. Electrochem. Soc.* **133** (1986) 1850.
[12] A. Storck, P. M. Robertson and N. Ibl, *Electrochim. Acta* **24** (1979) 373.
[13] F. Leroux and F. Coeuret, *Electrochim. Acta* **30** (1985) 159.
[14] A. Storck, M. A. Enriquez-Granados, M. Roger and F. Coeuret, *Electrochim. Acta* **27** (1982) 293.
[15] D. A. Cox and R. E. W. Jansson, *J. Appl. Electrochem.* **12** (1982) 205.
[16] S. H. Mohnot and E. L. Cussler, *Chem. Eng. Sci.* **39** (1984) 569.
[17] J. Wang, *Electrochim. Acta* **26** (1981) 1721.
[18] J. Comiti, Thèse de Doctorat d'Etat, I.N.P. de Grenoble, Grenoble, France (1987).